ELSEVIER

Ceramics International 26 (2000) 571–578

CERAMICS INTERNATIONAL

The microstructure of an yttria-doped hot-pressed silicon nitride

F.A. Costa Oliveira[1], P. Tambuyser, D.J. Baxter*

European Commission — Joint Research Centre, Institute for Advanced Materials, JRC Petten, PO Box 2, NL-1755 ZG Petten, The Netherlands

Received 8 March 1999; received in revised form 16 April 1999; accepted 15 September 1999

Abstract

A thorough knowledge of a material's microstructure is an essential starting point from which material development and property characterisation can be undertaken. This paper discusses the importance of combining different techniques, namely X-ray diffractometry, scanning electron microscopy and transmission electron microscopy for gaining a better understanding of the complex microstructure of commercially available Si_3N_4-based ceramics. Microstructural analyses of a commercial hot-pressed silicon nitride densified with the aid of 9.0 wt% Y_2O_3 and 1.7 wt% Fe_2O_3 revealed that this material consists primarily of prismatic hexagonal grains of β-Si_3N_4 surrounded by a crystalline intergranular phase identified as $Y_{10}(SiO_4)_6N_2$ (also known as H-phase), the volume fraction of which was estimated to be about 15%. By means of electron diffraction pattern analysis in a conventional TEM some pockets of $YNSiO_2$ (known as K-phase) were identified. TEM analyses also revealed that the material contains both iron silicides ($FeSi_2$) and silicon carbide (SiC) particles as inclusions.

Keywords: B. Electron microscopy; B. Grain boundaries; B. Inclusions; D. Si_3N_4

1. Introduction

In view of its outstanding high temperature properties (namely, good oxidation and thermal shock resistance), silicon nitride has long been regarded as one of the leading candidate materials for structural components in a number of applications, such as gas turbines or automotive engines [1]. Moreover, the low density of silicon nitride of 3200 kg m^{-3} (about 40% of the density of high temperature superalloys) offers the possibility of fabricating components of lower weight which can be used to achieve higher process efficiencies.

Dense, high strength Si_3N_4 materials can be produced by hot pressing via liquid phase sintering. The fabrication of dense Si_3N_4 ceramics normally requires a sintering additive because of the extremely low self-diffusivities in the covalently bonded α- and β-Si_3N_4 structures. Additions of metal oxides, e.g. MgO and Y_2O_3, participate in liquid phase formation at elevated sintering temperatures by the reaction of constituents above a eutectic temperature. The liquid promotes densification through a solution-reprecipitation mechanism and acts as a mass transport medium during densification [2]. The transport properties of the liquid phase are dependent on its volume fraction and chemistry. Upon cooling the liquid solidifies and forms secondary phases. The number, chemistry and volume fraction of the secondary phases depend on the starting powder constituents and temperature. Limitations to the potential high temperature applications of Si_3N_4-based ceramics are mainly related to the properties of the secondary phases formed on sintering. Indeed, subsequent exposure of these ceramics at high temperatures generally has an adverse effect on high-temperature mechanical and chemical properties owing to softening of residual glassy grain-boundary phases [2].

Nowadays, it is well recognised that silicon nitride densified with Y_2O_3 can result in the formation of highly refractory grain-boundary phases with improved high temperature behaviour compared with other sintering aids systems, e.g. MgO [3,4]. Although the use of Y_2O_3 produces significantly improved mechanical properties at high temperatures (>1300°C) compared with MgO-doped hot-pressed materials [3], some compositions of silicon nitride hot-pressed with >10 wt% yttrium oxide are prone to fail catastrophically around

* Corresponding author. Tel.: +31-224-565227; fax: +31-224-563841.

[1] Present address: Instituto Nacional de Engenharia e Tecnologia Industrial, Estrada do Paço do Lumiar, P-1699 Lisboa Codex, Portugal.

E-mail address: baxter@jrc.nl (D.J. Baxter).

0272-8842/00/$ - see front matter
PII: S0272-8842(99)00097-8

1000°C in oxidising environments despite their apparent stability at higher temperatures (e.g. 1400°C) [4,5]. Providing that the surface of the material is not completely covered by a protective SiO_2 layer, the unstable quaternary crystalline phases [$Y_{10}(SiO_4)_6N_2$, $Y_4Si_2O_7N_2$, $Y_2Si_3O_3N_4$ and $YSiO_2N$] formed on sintering (shown in the Si_3N_4–SiO_2–Y_2O_3 phase equilibrium diagram [4] in Fig. 1) can readily oxidise [4], resulting in substantial increases in molar volume (e.g. oxidation of $Y_2Si_3O_3N_4$ results in a molar volume change of 30%) [2]. This volume change can cause internal stresses to build up, resulting in cracking and eventual disintegration of the material. At temperatures typically higher than 1200°C, the problem of catastrophic oxidation is not observed owing to the rapid growth and softening of the surface silicate layer which contributes to relieving oxidation-induced stresses [5]. Therefore, careful selection of the composition of Si_3N_4-based materials densified with Y_2O_3 is required in order that formation of the undesirable secondary phases is avoided.

This paper focuses on the characterisation of the microstructure of a commercial hot-pressed Si_3N_4 with Y_2O_3 and Fe_2O_3, denoted Ceranox NH209 and illustrates the importance of combining several techniques, e.g. XRD, SEM and TEM in order to identify the different secondary phases present in the Si_3N_4-based material.

2. Experimental

2.1. Material

The material used in the present investigation was Ceranox NH209 (ex Feldmühle AG, now Ceramtec, Germany), a dense (3330 kg m^{-3}) hot pressed (40 MPa at 1750°C) silicon nitride with a porosity content of 2 vol%. According to the manufacturer, this material contains 9.0 wt% Y_2O_3 and 1.7 wt% Fe_2O_3, as well as traces of Al_2O_3 (0.12 wt%), CaO (0.05 wt%), MgO (0.01 wt%) and ZrO_2 (0.01 wt%) as major impurities.

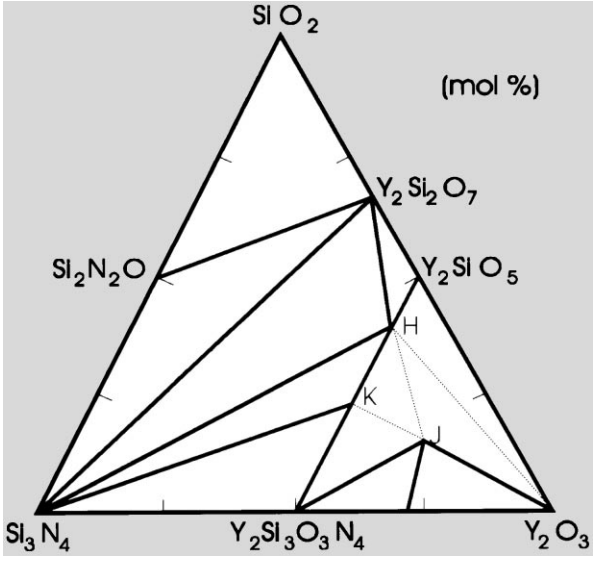

Fig. 1. Phase equilibrium diagram of Si_3N_4–SiO_2–Y_2O_3 at 1823 K (where H = $Y_5(SiO_4)_3N$; J = $Y_4Si_3O_7N_2$ and K = $YSiO_2N$) [4].

2.2. Microanalysis

The microstructure of Ceranox NH209 was characterised by X-ray diffractometry (XRD), scanning electron microscopy (SEM) and transmission electron microscopy (TEM).

XRD analyses were carried out using a Philips APD 1700 automated powder diffractometer. The as-received material was analysed in the solid form (owing to its high hardness, milling would have introduced contaminants). Samples were analysed using monochromatic copper radiation with wavelength $K_\alpha = 1.542$ Å. Analysis of the diffraction patterns was computer assisted by comparing the calculated '*d*' (spacing of crystal planes) values and relative intensities with those listed in the library of reference spectra of the Joint Committee on Powder Diffraction Standards (JCPDS). Difficulties in the interpretation of XRD data arise from the number of crystalline phases present, overlapping of reflections, roughness of sample surface, the amount (detection limit ≈5 wt%) and preferential orientation of the phases present as well as uncertainties in the phase composition of the reference materials quoted in the JCPDS system.

Polished sections of Ceranox NH209 were examined using back-scattered electrons in a Zeiss DSM 940 scanning electron microscope equipped with an energy dispersive X-ray spectroscopy analyser (EDX - KEVEX Sigma) for qualitative elemental analysis. The back scattered electron (BSE) imaging technique was applied in order to take advantage of differences in the atomic numbers of the elements constituting the different phases. Prior to examination, the samples were embedded in an epoxy resin and polished with a series of diamond pastes to a 1 μm finish. Since the silicon nitride material under investigation was non-conducting, it was necessary to coat it with a thin layer of carbon to prevent surface charging during examination.

Although observations on a section through the microstructure does not reveal true information about the three-dimensional structure, image analyses were carried out on polished cross-sectional images of as-received material, obtained by SEM using Zeiss Kontron KS 400 software, in order to assess the fraction of secondary phase present in the material.

Foils for TEM were prepared from slices of thickness 0.2–0.5 mm, cut with a diamond saw. Discs were drilled out ultrasonically, hand ground to a thickness of around 25 μm and finally ion-milled to electron

transparency with 6 kV argon ions incident on the surface at 18°. Prior to examination, the thinned foils were coated with evaporated carbon to prevent charging under the electron beam. Two specimens, from different batches were examined in a transmission electron microscope (Philips EM 400T) at 120 kV. For studying intergranular phase pockets, conventional dark/bright field techniques were applied. Phase identification was carried out by selected area electron diffraction and micro/convergent beam diffraction and EDX (KEVEX) microanalysis of elements with an atomic number higher than 11.

3. Results and discussion

3.1. General structure/homogeneity

SEM of polished sections of Ceranox NH209 showed that the microstructure of this material (as shown in Fig. 2) consists of two main phases: the silicon nitride matrix (dark grey areas) and the secondary phases (white areas). In addition, pores (black spots) and inclusions (finely dispersed in the matrix), were observed. These inclusions (not visible in Fig. 2 due to their brightness being similar to that of the other secondary phases) were found by EDX to be iron-rich (presumably $FeSi_2$, as found by TEM). XRD analysis showed the main crystalline phase present to be β-Si_3N_4. XRD also revealed that there was no significant difference in the diffraction patterns obtained for samples from two different batches, indicating that the material was homogeneous from batch to batch. Homogeneity was also confirmed by both SEM and TEM analyses.

Despite the material's apparent homogeneity, SEM analyses revealed that this material has a broad grain size distribution (grain thickness ranging from 0.1 to 5 μm and grain length as large as 20 (m), which is typical of this kind of ceramic [6]. Some of the grains were sectioned normal to the *c*-axis and therefore appear roughly hexagonal, whereas others were sectioned parallel to the *c*-axis, revealing a prismatic shape. It was also observed that the intergranular phase was rather 'heterogeneously' distributed in the bulk (large pockets are often seen surrounding smaller Si_3N_4 grains) as clearly shown in Fig. 2. The majority of the bright areas in the BSE image correspond to the high yttrium containing phases in Ceranox NH209. The area fraction of grain-boundary phase present in this material was estimated to be $15 \pm 1\%$, using an automatic image analysis system with 10 images randomly chosen over a polished surface, and assuming the material to be isotropic.

The type and amount of metal oxides used as sintering aids determines the temperature at which the first liquid is formed as well as the volume fraction and viscosity of the liquid phase that forms during densification. The viscosity of oxynitride glasses is expected to increase with yttrium content [7]. An increase in viscosity of the liquid phase formed on sintering should reduce the rate of shrinkage during the particle rearrangement stage and will also reduce the material transport through the liquid. This may explain the occurrence of some porosity, which is particularly evident in regions of lower intergranular phase content, as illustrated in Fig. 2 (pores correspond to the dark spots in this figure). Another possible explanation for this finding is that the mixing step did not result in an 'ideally' uniform distribution of the sintering aids. In any case, the small scatter obtained in quantifying the area fraction of the intergranular phase suggests that the overall microstructure is rather homogeneous.

3.2. Secondary/intergranular material characterisation

In previous work [8], it has been reported that Ceranox NH209 contains prismatic hexagonal grains of β-Si_3N_4

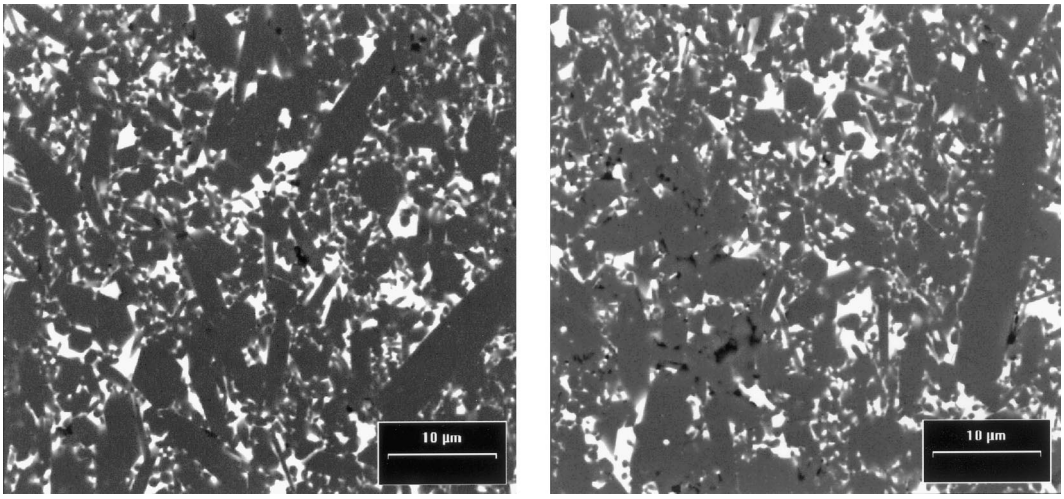

Fig. 2. BSE images of polished cross-sections of Ceranox NH209.

(some of which were up to 17 μm long [9]) surrounded by a crystalline phase of yttrium nitrogen apatite structure, identified as $Y_{10}(SiO_4)_6N_2$ (also known as H-phase). This phase can accommodate impurities (particularly Ca, Al and Mg) in solid solutions, which would otherwise form a low softening-temperature glass leading to the degradation of the high temperature properties [10]. Other reports, however, also mention that, in addition to H-phase, another phase, possibly $YSiO_2N$ (known as K-phase) may also be present [11].

Analysis of the XRD patterns obtained in this work for Ceranox NH209 showed that the crystalline components of the secondary phase were Y–N-apatite ($Y_{20}N_4Si_{12}O_{48}$), also known as H-phase, and possibly Y–N-wollastonite ($YSiO_2N$), known as K-phase. However, the latter could not be ascribed with certainty due to overlapping of reflections of H- and K-phases. Therefore, a detailed study of the intergranular phase present in the material by means of transmission electron microscopy (TEM) was carried out for the purpose of clarification.

TEM evidence indicates that the pockets of secondary phases found mainly at three- or four-grain junctions were crystalline (no amorphous phase could be seen under the magnifications used, typically 60 000×). This does not necessarily mean that the material is fully crystalline. Recent work, both theoretical and experimental, has revealed the existence of an equilibrium film thickness, between adjacent Si_3N_4 grains, which has been found to depend on the chemical composition of the liquid phase in these materials rather than on its amount [12]. In fact, theoretical modelling [13] based on two continuum approaches, one based on interfacial energies and the other on the force balance normal to the grain boundary, postulate that there is an equilibrium thickness of the grain boundary film at Si_3N_4/Si_3N_4 interfaces. The equilibrium film thickness (which is of the order of 1 nm) [13] is a result of two competing interactions; an attractive van der Waals interaction between the grains on either side of the boundary and a repulsive interaction due to the structure of the intergranular liquid. This has been confirmed experimentally for Si_3N_4 densified with a variety of metal oxide additives, with the film thickness ranging from 0.5 to 2.0 μm, depending on the additive [12,13,14].

Both theoretical and experimental works have in fact shown that there is a critical volume of the intergranular phase pocket for crystallisation to be energetically favourable [15]. Even if it is assumed that the composition of the smaller glassy regions is similar to that of larger pockets, mechanical constraints from the surrounding crystalline material oppose crystallisation. The reason is that any volume change during phase transformation leads to a strain energy, which hinders the transformation. The evidence that small glassy pockets and thin amorphous intergranular films in Si_3N_4 remain undevitrified after heat-treatments supports this fact [15]. This is in agreement with the predictions of Raj and Lange [16]. Based on both thermodynamic and kinetic considerations, they postulated that as the pocket of grain boundary phase becomes smaller, crystallisation becomes increasingly difficult [16].

The composition of the oxynitride liquid phase [17], the temperature-time history [18,19], e.g. the undercooling below the solidus temperature [20], and the cooling rate, are other factors affecting crystallisation. Indeed, a thermodynamic barrier for crystallisation can be generated. This could be achieved by altering the chemistry of the intergranular phase to a composition with slow crystallisation kinetics, or by the introduction of internal stresses originating from volume changes during crystallisation and due to thermal effects on cooling.

The influence of these parameters on the microstructure of Ceranox NH209 could not be reliably established owing to the lack of information regarding the sintering temperature-time history. The analysis of thin intergranular films of residual liquid phase (as seen in Fig. 3) which are present throughout the microstructure between adjacent Si_3N_4 grains was inconclusive due to lack of resolution. Further analytical work by means of high resolution electron microscopy will be necessary to fully establish the size and the chemistry of the very thin films seen at 2-grain junctions, as reported by other authors [12,14,19–22].

Most pockets of intergranular phase, which occasionally partially enveloped silicon nitride grains (Fig. 4), were identified by means of selected area electron diffraction as $Y_{10}(SiO_4)_6N_2$ (as indicated by the spot spacings of the electron diffraction pattern inset shown in Fig. 5 that were found to correspond closely with those reported for H-phase). This is consistent with the XRD phase identification (JCPDS card: 30-1462).

Wills et al. [22] reported that this quaternary crystalline phase ($10Y_2O_3{\cdot}9SiO_2{\cdot}Si_3N_4$) has a hexagonal unit cell ($a = 9.436$ Å and $c = 6.822$ Å). It has been suggested that this phase is isostructural with fluoroapatite, i.e. $Ca_5F(PO_4)_3$ ($a = 9.368$ Å, $c = 6.881$ Å) and thus may be represented by the formula $Y_5N(SiO_4)_3$ [22]. Other authors [4], however, have represented this phase as $5Y_2O_3{\cdot}4SiO_2{\cdot}Si_3N_4$ ($Y_{10}Si_7O_{23}N_4$). This difference may be a result of the capability of the rare-earth apatite phases ($Ln_{8+2x+0.67y}(SiO_{4-x}N_x)_6O_y$, where $0 \leqslant y \leqslant 2$ and $0 \leqslant 2x + 0.67y \leqslant 2$)[2] to accommodate appreciable amounts of impurities (always present in the starting silicon nitride powders) in solid solution. It is therefore not surprising that the exact composition of the H-phase is still a matter of controversy. However, the present observations are in good agreement with the diffraction pattern reported by Wills et al. [22].

Larger pockets of H-phase often contained Si_3N_4 grains with small and rounded edges, and the Si_3N_4

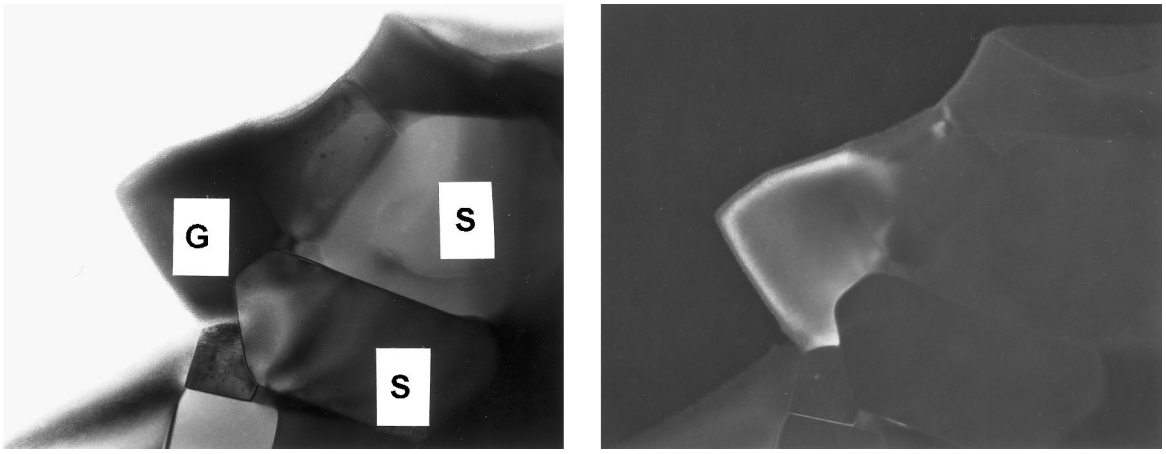

Fig. 3. Crystalline pocket of grain boundary phase (G) imaged in bright field (BF, left) and dark field (DF, right) and typical thin film which separates individual Si_3N_3 (S) grains (magnification 60 000).

grains surrounding such pockets had either a rounded or faceted shape. This suggests that a solution/reprecipitation process occurred during densification. Rounded sections must have resulted from dissolution in the liquid phase medium, whereas grains with faceted sections probably grew from the liquid phase developing a prismatic shape [17,23].

The present investigation clearly confirmed the presence of $YSiO_2N$ (known as K-phase). Making use of standard selected area diffraction, electron diffraction patterns (Fig. 6) enabled identification of K-phase in some grain-boundary pockets that contained striations. The striation feature, although not always present, made it easier to distinguish K-phase from H-phase pockets (Fig. 7). The source of striations is probably related to stacking faults along the *c*-axis hexagonal pseudo sub-cell, which is typical of wollastonite structures [26]. Morgan et al. [24] concluded that $YSiO_2N$ belongs to the pseudo-wollastonite structures of the $CaSiO_3$ type, and has a monoclinic unit cell in which there exists a strong hexagonal pseudo sub-cell ($a = 7.02$ Å, $c = 9.10$ Å). The X-ray diffraction pattern for $YSiO_2N$ obtained by Morgan et al. [24] is different from that reported by Lange et al. [2]. This may be due to difficulties in producing pure $YSiO_2N$ as demonstrated by O'Reilly's work [25]. In fact, traces of J-phase ($Y_4Si_2O_7N_2$) were always found to be present in the samples prepared by O'Reilly, suggesting that it is difficult to obtain 'pure' $YSiO_2N$ phase. Therefore, the differences between the X-ray diffraction patterns found in the literature are possibly related to the degree of purity of the phases examined by the different authors.

3.3. Inclusions

The presence of $FeSi_2$, indicated by the material's manufacturer and confirmed by Veyret [8,9], could be ascribed with certainty by means of selected area electron diffraction and EDX microanalysis carried out on the TEM. In fact, electron diffraction patterns revealed that particles of irregular shape and mottled surface contrast found by EDX to contain Si and Fe (with sizes ranging from 0.6 to 1.4 μm) were consistent with $FeSi_2$ (JCPDS card: 20-0532). Iron is thus largely concentrated in the small particles shown in Fig. 8.

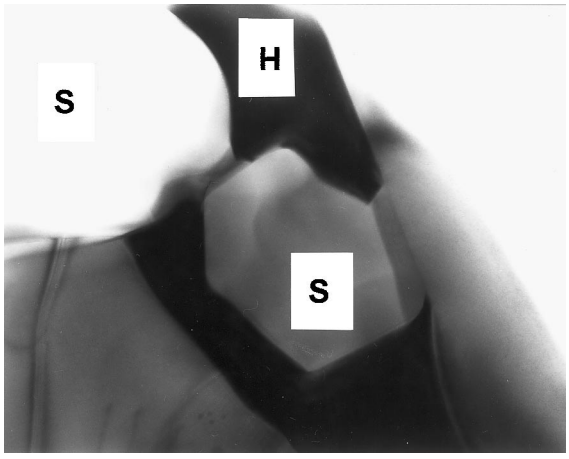

Fig. 4. Bright field TEM micrograph of crystalline pockets of grain boundary H-phase (H) partially enveloping a Si_3N_4 (S) grain (magnification 60 000).

The use of transition metal oxides such as chromium(III) oxide (Cr_2O_3) and iron(III) oxide (Fe_2O_3) has been investigated by Godfrey [27] and their addition appears to aid the densification process, although the exact mechanism is not clearly understood [28]. These oxides usually react to form silicides such as MSi or MSi_2, where M denotes the transition metal. Iron is also a common impurity in silicon nitride powders, but contamination can also be introduced during the milling process. Iron(III) oxide melts at 1566°C and does not form any compound with SiO_2 [28]. At high temperature, under reducing conditions (i.e. low oxygen partial

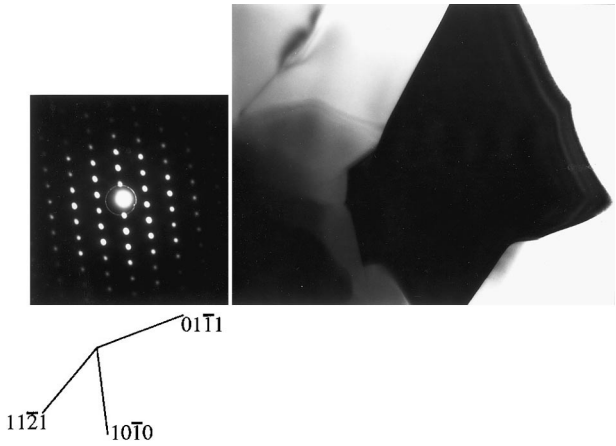

Fig. 5. Bright-field TEM micrograph of a pocket of grain-boundary H-phase with electron diffraction pattern: [$\bar{1}2\bar{1}3$] zone axis (magnification 60 000).

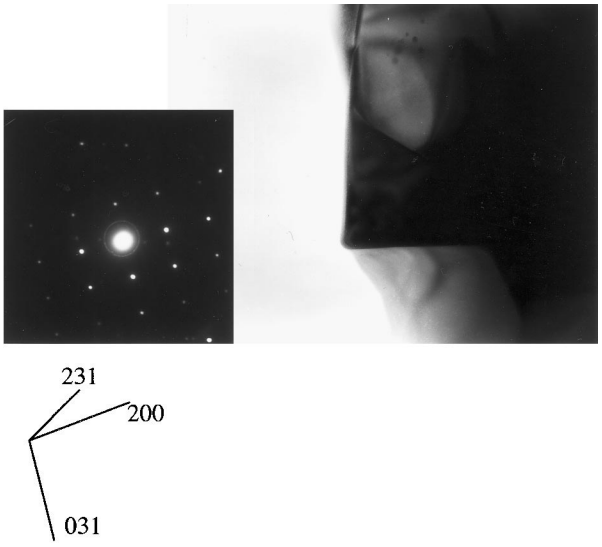

Fig. 6. Bright-field TEM micrograph showing a pocket of grain-boundary K-phase with the electron diffraction pattern: [0$\bar{1}$3] zone axis (magnification 60 000).

pressure), iron(III) oxide reduces to iron(II) oxide (which melts at 1370°C). Iron(II) oxide can react with the silicon dioxide present on the surface of silicon nitride powders to form fayalite (Fe_2SiO_4), which melts at 1205°C. It can be inferred that the appearance of a liquid phase at temperatures as low as 1200°C is expected to contribute to the densification of silicon nitride. Another important function of the transition metal oxide is to produce additional SiO_2 from the reaction with Si_3N_4, according to the reaction:

$$2M_2O_3(s) + Si_3N_4(s) \leftrightharpoons 3SiO_2(s) + 6M(s) + 2N_2(g) \quad (1)$$

that may be beneficial in generating a larger volume of transient liquid phase. Iron released by the reduction of the oxides can react with Si_3N_4 to form silicides [28]

Fig. 7. Bright field TEM micrograph of a crystalline pocket of K-phase showing light and dark striations which were observed in many triple points (magnification 60 000).

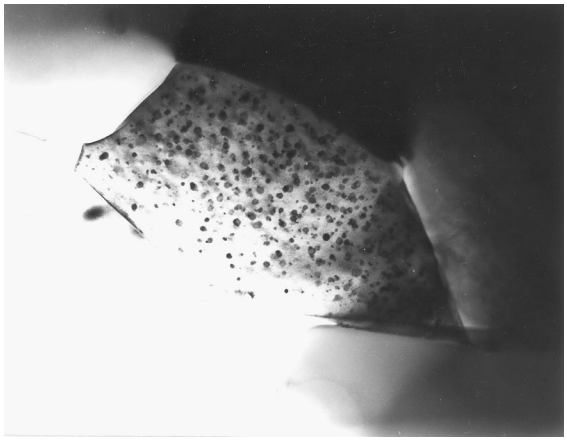

Fig. 8. Bright-field TEM micrograph showing a $FeSi_2$ particle (magnification 60 000).

$$Fe(s) + x/3Si_3N_4(s) \leftrightharpoons FeSi_x(l) + x/6N_2(g) \quad (2)$$

The formation of these silicides leads to the appearance of isolated liquid globules ultimately yielding particulate inclusions embedded in the intergranular phase of the silicon nitride.

In addition, round particles ranging from 200 to 750 nm in size (Fig. 9) and containing planar defects, were found by EDX to be silicon-rich. Their electron patterns were also consistent with hexagonal silicon carbide (JCPDS card: 29-1131) ($a = 0.307$ nm and $c = 1.508$ nm). The presence of SiC inclusions is attributable to the pick-up of carbon from graphite hot-pressing dies used during manufacture. Finally, other numerous intragranular inclusions inside the Si_3N_4 grains were observed (Fig. 10). These rounded particles, in the size range 40 to 80 nm, could not be identified using the techniques available.

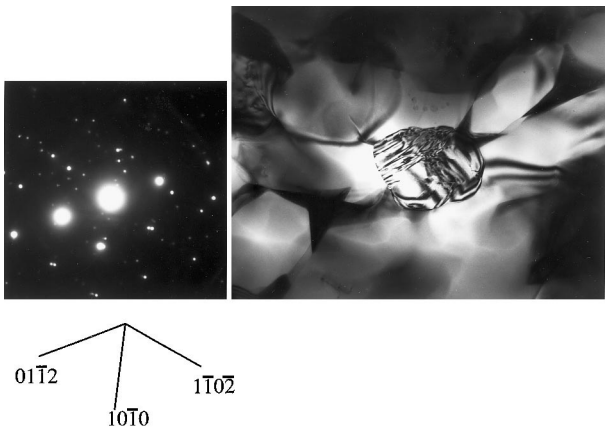

Fig. 9. Bright-field TEM micrograph showing a SiC particle with electron diffraction pattern: [02$\bar{1}$] zone axis (magnification 60 000).

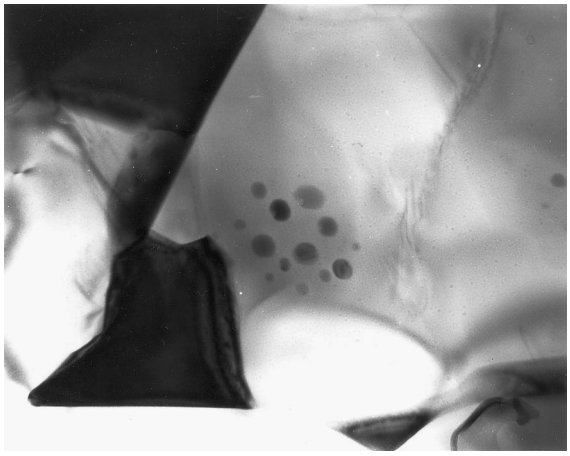

Fig. 10. Bright-field TEM micrograph showing small intragranular inclusions (magnification 60 000).

4. Concluding remarks

The main conclusions, which may be made following an investigation of the microstructure of the Y_2O_3 hot-pressed silicon nitride investigated (Ceranox NH209), are:

1. The complex microstructure of Ceranox NH209 consists of β-Si_3N_4 grains and secondary phases that result from the reaction of SiO_2 (always present on the surface of Si_3N_4 starting powders) and the densification aids (e.g. Y_2O_3 and Fe_2O_3). Experimental evidence gathered by means of conventional transmission electron microscopy has confirmed that the grain-boundary phase pockets (usually seen at three- or four-grain junctions) consist of both H- (major) and K- (minor) phases. It is thus apparent that the composition of Ceranox NH209 should fall within the Si_3N_4–$YSiO_2N$–$Y_5(SiO_4)_3N$ phase compatibility triangle.
2. All impurities, except iron, were incorporated in solid solutions, thus explaining why apparently no pockets of amorphous intergranular phase were observed by TEM at 3- or 4-grain junctions.
3. Thin intergranular films, most likely amorphous, present throughout the microstructure between adjacent Si_3N_4 grains were too thin (less than 5 nm) to be analysed using the instruments available. Further analytical work by means of high resolution electron microscopy is needed to determine the size and chemistry of these thin films seen at 2-grain junctions.
4. This paper highlights the importance of combining different analytical techniques in order to enable a more complete characterisation of the complex microstructure of commercially available silicon nitrides.

Acknowledgements

One of the authors (FCO) wishes to thank the European Commission for a post-doctoral fellowship. We wish to thank P. Moretto, J. Van Eijk, P. Frampton and K. Schuster for their valuable assistance. This work was carried out within the European Commission's Research and Development Programme.

References

[1] G. Wötting, L. Frassek, G. Leimer, L. Schönfelder, Application-oriented development of high-performance-Si_3N_4 materials and components, Cfi/Ber.DKG 70 (1993) 1–8.
[2] F.F. Lange, Silicon nitride polyphase systems: fabrication, microstructure, and properties, International Metals Reviews 25 (1980) 1–20.
[3] G.E. Gazza, Hot-pressed Si_3N_4, J. Am. Ceram. Soc. 56 (1973) 662.
[4] F.F. Lange, S.C. Singhal, R.C. Kuznicki, Phase relations and stability studies in the Si_3N_4–SiO2–Y_2O_3 pseudoternary system, J. Am. Ceram. Soc. 60 (1977) 249–252.
[5] J.K. Patel, D.P. Thompson, The low-temperature oxidation problem in yttria-densified silicon nitride ceramics, Br. Ceram. Trans. J. 87 (1988) 70–73.
[6] H. Björklund, J. Wasén, L.K.L. Falk, Quantitative microscopy of β-Si_3N_4 ceramics, J. Am. Ceram. Soc. 80 (1997) 3061–3069.
[7] S. Hampshire, R.A.L. Drew, K.H. Jack, Viscosities, glass transition temperatures, and microhardness of Y–Si–Al–O–N glasses, J. Am. Ceram. Soc. 67 (1984) C46.
[8] J.B. Veyret, R.J. Fordham, M. Billy, Influence of oxidation in SO_2–air mixtures on the room-temperature strength of silicon nitride, J. Eur. Ceram. Soc. 13 (1994) 313–321.
[9] J.B. Veyret, Comportement à l'oxydation de céramiques à base de nitrure de silicium en atmosphère complexe air/SO_2. Ph.D. thesis, University of Limoges, France, 1989.
[10] A.W.J.M. Rae, D.P. Thompson, K.H. Jack, The role of additives in the densification of nitrogen ceramics, in: J.J. Burke, E.N. Katz, R.N. Katz (Eds.), Ceramics for High Performance Applications — II, Brook Hill Publishing Company, Chestnut Hill, MA, 1978, pp. 1039–1067.

[11] R.J. Fordham, J.F. Norton, S. Canetoli, J.F. Coste, In situ studies of the surface changes occurring during high-temperature oxidation of silicon nitride, in: S.B. Newcomb, M.J. Bennett (Eds.), Microscopy of Oxidation 2, The Institute of Materials, London, 1993, pp. 545–554.
[12] C.M. Wang, X. Pan, M.J. Hoffmann, R.M. Cannon, M. Rühle, Grain boundary films in rare-earth-glass-based silicon nitride, J. Am. Ceram. Soc. 79 (1996) 788–792.
[13] D.R. Clarke, On the equilibrium thickness of intergranular glass phases in ceramic materials, J. Am. Ceram. Soc. 70 (1987) 15–22.
[14] G. Pezzotti, K. Ota, H.J. Kleebe, Grain-boundary relaxation in high-purity silicon nitride, J. Am. Ceram. Soc. 79 (1996) 2237–2246.
[15] L.K.L. Falk, G.L. Dunlop, Crystallization of the glassy phase in an Si_3N_4 material by post-sintering heat treatments, J. Mat. Sci. 22 (1987) 4369–4376.
[16] R. Raj, F.F. Lange, Crystallization of small quantities of glass (or a liquid) segregated in grain boundaries, Acta Metallurgica 29 (1981) 1993–2000.
[17] E.M. Knutson-Wedel, L.K.L. Falk, H. Björklund, T. Ekström, Si_3N_4 ceramics formed by HIP using different oxide additions — relation between microstructure and properties, J. Mat. Sci. 26 (1991) 5575–5584.
[18] H. Kessler, H.-J. Kleebe, R.W. Cannon, W. Pompe, Influence of internal stresses on crystallisation of intergranular phases in ceramics, Acta Metall. Mater. 40 (1992) 2233–2245.
[19] C. Wang, H. Emoto, M. Mitomo, Nucleation and growth of silicon oxynitride grains in a fine-grained silicon nitride matrix, J. Am. Ceram. Soc. 81 (1998) 1125–1132.
[20] R. Raj, Morphology and stability of the glass phase in glass-ceramic systems, J. Am. Ceram. Soc. 64 (1981) 245–248.
[21] D.R. Clarke, G. Thomas, Microstructure of Y_2O_3 fluxed hot-pressed silicon nitride, J. Am. Ceram. Soc. 61 (1978) 114–118.
[22] R.R. Wills, S. Holmquist, J.M. Wimmer, J.A. Cunningham, Phase relationships in the system Si_3N_4–Y_2O_3–SiO_2, J. Mat. Sci. 11 (1976) 1305–1309.
[23] L.L. Wang, T.Y. Tien, I.-W. Chen, Morphology of silicon nitride grown from a liquid phase, J. Am. Ceram. Soc. 81 (1998) 2677–2686.
[24] P.E.D. Morgan, P.J. Carroll, F.F. Lange, Crystal structure of $YSiO_2N$ and a reappraisal of the 'vaterite' type YBO_3, Mat. Res. Bull. 12 (1977) 251–259.
[25] M. O'Reilly, The high temperature corrosion behaviour of intergranular phases of silicon nitride. Ph.D. thesis, University of Dublin, 1995.
[26] S.A. Bradley, K.R. Karasek, Analysis of grain boundaries for reaction-bonded silicon nitride with yttria addition, J. Mat. Sci. Lett. 6 (1987) 791–794.
[27] D.J. Godfrey, Fabrication, formulation, mechanical properties, and oxidation of sintered Si_3N_4 ceramics using disc specimens, Mat. Sci. Techn. 1 (1985) 510–515.
[28] A.D. Stalios, J. Luyten, C.D. Hemsley, F.L. Riley, R.J. Fordham, The interaction of iron during the hot-pressing of silicon nitride, J. Eur. Ceram. Soc. 7 (1991) 75–81.